

Bending tests on circular braided ropes under variation of different peripheral test conditions

Christoph Müller^{1*}, Andreas Kretschmer¹, Piia Koskenjoki², Kirsi Saarinen-Pulli², Markus Golder¹

¹ Chemnitz University of Technology, Professorship of Conveying Engineering and Material Flow Technology, Chemnitz, DE-09116, Germany

² Konecranes, Hyvinkää, FI-05830, Finland

* Correspondence: christoph.mueller@mb.tu-chemnitz.de; Tel.: +49-371-531-37989

Peer reviewed article

Received 17 October 2024; Revised 11 December 2024; Accepted 13 December 2024; Available online December 2024

© 2024 by C. Müller and the other authors. This is an open access article distributed under the Creative Commons Attribution License (CC-BY 4.0), which permits unrestricted use, distribution, and reproduction in any medium, provided the original work is properly cited. The innoTRAC logo and third-party content are excluded from this.

ABSTRACT Various companies are working on the utilisation of high performance fibre ropes (HPFR) in industrial cranes and conveyor systems. In a collaboration between Konecranes and TUC, application-relevant influencing variables on bending wear were investigated experimentally. This paper summarizes these test results from single cyclic bending over sheave (CBOS) tests on circular braided ropes. The ropes investigated are single-ply, uncovered circular (round) braided ropes made of UHMW-PE yarns. The ropes are industrially manufactured and have a coating. Different factor levels were varied as part of the investigations. These are i) the line pull (referred to as safety factor S_f), ii) the angle of entry of the rope on the test sheave (referred to as fleet angle β_f), iii) the test sheave material (variation between polyamide PA and steel ST sheaves), iv) the bending ratio BV (as the ratio of the uncoiling diameter D to the rope diameter d) and v) the ambient temperature in the bending zone (referred to as T_{BZ} in the following). Finally, the results are compared and a known service life model is applied.

KEYWORDS fibre rope, crane, braid, CBOS, UHMW-PE

1. Introduction

Bending wear is known to occur in ropes running over sheaves. This is due to the differential bending diameters over the rope diameter and the resulting inevitable displacements of individual rope elements (strands, wires, fibres, etc.) against each other. These displacements under contact pressure cause corresponding frictional wear. In this respect, it is clear that the main factors influencing the wear rate are the D/d -

ratio (BV) and the existing static load. This does not differ between fibre and steel wire ropes. Accordingly, service life equations (see [NOV2017]), as found for steel wire ropes, are also applicable to fibre ropes. In addition to the bending wear, other damage mechanisms also occur depending on the application, such as friction of the outer strands against sheave flanks, internal friction and contact pressure due to dynamical loading and unloading as well as thermal or abrasive influences. In the present application of industrial hoists (see Figure 1), the D/d ratios are significantly lower than 40, diagonal pull can occur (results in a fleet angle deviation between rope axis and sheave plane) and thermal influences cannot be ruled out.



Figure 1: Utilisation of a fibre rope in an industrial crane (courtesy of Konecranes)

For simple single-ply circular braids made of High Modulus – High Tenacity (HM-HT) fibres, peripheral influences have already been investigated and published. For example in [VOG2004], [HEI2013] and [NOV2017]. The service lives of UHMW-PE round braided ropes in the CBOS test is a function of the strand load. It is obvious that the service life of the ropes in the tests decreases with increasing strand load. Furthermore, the influence of the D/d -ratio on the service life has already been investigated and published (see [VOG2004], [WHR2017]). Here it can be seen that the service life also decreases with decreasing D/d -ratio. The influence of increased ambient temperatures on the service life in the CBOS test, particularly for UHMW-PE ropes, is also known (see [ODN1032]). Various service life models are known and summarized, for example in [NOV2017]. The common logarithmic or double logarithmic representation must be critically evaluated. This is certainly helpful for engineers when dimensioning, but in a scientific context it can lead to misjudgements of effect sizes (e.g. of variances within a factor level). Accordingly, the author only uses linearly scaled axes in the illustrations. The aim of the recent series of experiments was to determine the respective effect sizes of the factor variation for specific rope variants. The variation of the factor levels is approximated to realistic ranges resulting from the application.

2. Experimental Setup

In the present measurement campaign, comparable ropes from various manufacturers were examined (see Table 1). All ropes were 12-stranded, without a protective cover and with a coating. The nominal diameter of the ropes was always specified as 8.5 mm, although their actual diameter deviated significantly from this specification in some cases.

Table 1: rope types used for experiments

rope type	weight per length in g/m	experimental* breaking force in kN	calculated** fibre cross section in mm ²	rope efficiency*** in kN/g/m	theor. Diameter**** in mm
1	44.8	71.6	45.5	1.59	7.61
2	35.9	54.9	36.6	1.53	6.83
3	44.4	68.5	45.3	1.154	7.59

* acc. ISO 2307

** derived by length and weight measurement

***relation of experimental breaking force per weight per length

****calculated from fibre cross section and density of fibre

Various series of measurements were carried out. Table 2 provides an overview of the factors and factor levels. The series of measurements were planned and carried out with nominal line pull and nominal bending ratio. However, the real safety factors and bending ratios are given in Table 2 for better evaluation. In test series 1, two comparable ropes were tested with varying line loads. In measurement series 2, the bending ratio between the two test sheaves (see Table 3) is compared. In measurement series 3, different fleet angles are evaluated as a function of the bending ratio and the sheave material. Furthermore, the long-term behaviour of the polyamide test sheave is evaluated. In measurement series 4, the behaviour of two comparable ropes at elevated temperatures in the bending zone is investigated.

All series of measurements were carried out on the same CBOS testing machine (see Figure 2), which enables a maximum line pull of 50 kN. The line pull F_s is applied to the test disk assembly by a jackscrew drive (1) and controlled during the test. The control hysteresis was set to 3 % for this study. An individual test disks (2) can be applied to the upper test shaft. The rotary movement is initiated by means of the lower drive sheave (3). For the tests with increased temperature in the bending zone, a temperature-controlled chamber was attached to the test sheave.

Table 2: Factors and factor levels of the measurement series

	factor	factor level number	rope type	safety factor (S_F)	bending ratio (BV)*	sheave material	temp. bending zone (T_{BZ})	fleet angle (β_f)
Series 1a	S_f	6	1	2.4 2.9 4.6 5.7 7.6 11.5	22.5	ST	RT**	0°
Series 1b	S_f	6	2	1.8 2.2 3.5 4.4 5.9 8.8	25.1	ST	RT	0°
Series 2	BV	2	1	5.7	16.8 22.5	PA ST	RT	0°
Series 3a	β_f	5	1	5.7	16.8	PA	RT	0° 1° 2° 3° 4°
Series 3b	β_f	5	1	5.7	22.5	ST	RT	0° 1° 2° 3° 4°
Series 3c	β_f	1	1	5.7	16.8	PA	RT	4°
Series 4a	T_{BZ}	7	1	5.7	22.5	ST	RT 30 °C 40 °C 50 °C 60 °C 70 °C 80 °C	0°
Series 4b	T_{BZ}	7	3	5.8	22.6	ST	RT 30 °C 40 °C 50 °C 60 °C 70 °C 80 °C	0°

* related to theoretical rope Diameter in Table 1.

** RT is test at room temperature without temp. control

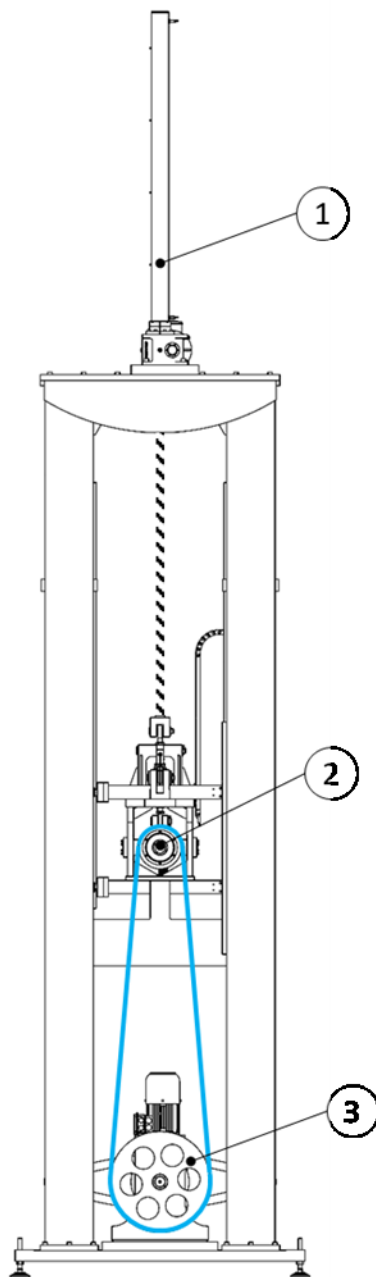


Figure 2: Schematic diagram of the TUC-WBM-50-1 bending machine

The bending ratio on the drive sheave is always significantly higher than that of the test sheaves (see Table 3). This means that the predominantly damaged area always occurs in the rope area running over the test sheave. The parameterization of the CBOS test includes the bending test length l_p and the bending frequency in addition to the factor levels such as line load and D/d -ratio. In conjunction with other geometric factors (see Figure 3), the bending test length defines the length of the completely alternately bent and thus damaged area l_1 of the rope (see Equations 1 and 2). The length of this area should be at least greater than the lay or braid length.

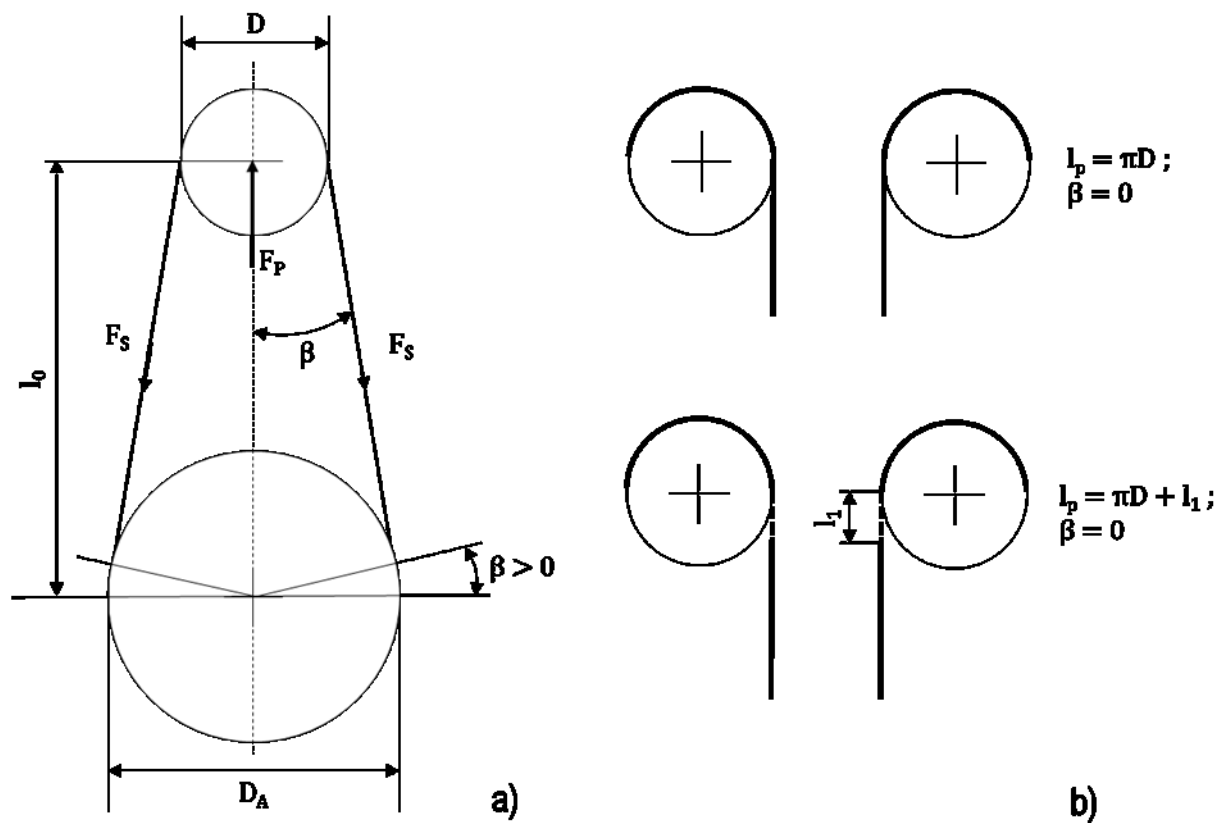


Figure 3: Schematic diagram of the geometric conditions on a bending machine, a) total view of rope on bending machine, b) start and end positions of the bending zone for different bending length

$$\beta = \arctan \frac{D_A - D}{2l_0} \quad (1)$$

$$l_1 = l_p - D(\pi - 2\beta) \quad (2)$$

Table 3: Geometric setup of the CBOS test

Parameter description	Symbol	Value
Test sheave diameter in the groove base	D	127.5 mm (PA-Sheave) 171.5 mm (Steel-Sheave)
Drive pulley diameter in the groove base	D _A	500 mm
Center distance test pulley, drive pulley	l ₀	3,100 mm
Groove radius test sheave	r _R	4.4 mm
rope Angle to vertical	β	3.4° und 3.0°
Bending test length set	l _p	800 mm
Damaged length	l ₁	415 mm und 279 mm

A relatively low bending frequency of 10/min was set to prevent the UHMW-PE ropes from heating up and thus having an undesirable influence on the results. The surface temperature of the ropes in the bending zone was measured using a pyrometer while the test was being carried out. The surface temperature of the bending zone did not

exceed 30 °C during the entire measurement campaign for those which were tested at room temperature. The pyrometer measurement was validated with a corresponding contacting sensor on the rope surface before the start of the test. The groove geometry of the test sheaves is based on DIN 15061 with a round groove of 4.4 mm radius and an opening angle of 60 ° for ropes with a nominal diameter of 8.5 mm. The actual diameter of the tested ropes varies according to their design. The ropes were spliced end-to-end to form a test specimen and placed on the machine. The CBOS tests were carried out until the rope broke completely. This is detected by the control system by means of a drop of line pull when the rope breaks.

3. Results

The results of the various series of measurements are compared below. In Series 1a&b, two comparable ropes were tested in bending fatigue to rupture at different safety factors (see Chapter 2). As expected, the number of single bends (N) that can be sustained until failure also increases with increasing safety factor (see Figure 4 and Figure 5). N increases progressively with increasing safety factor. It can also be observed that the scatter of the repeated measurements at a load level also increases with increasing safety factor.

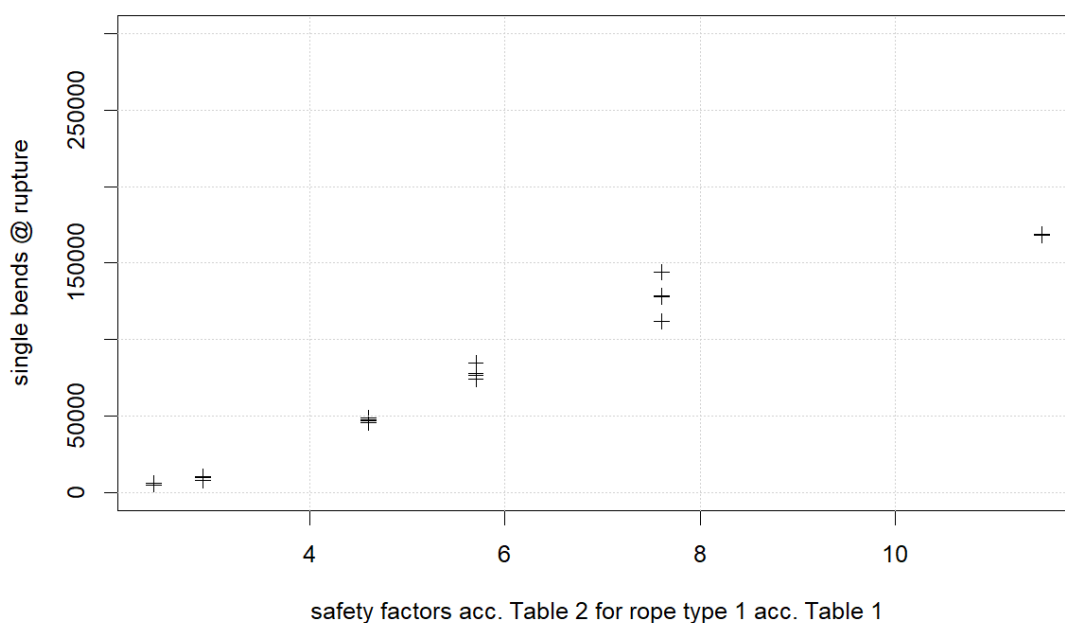


Figure 4: Series 1a, single bends to rupture for rope type 1 at various safety factors

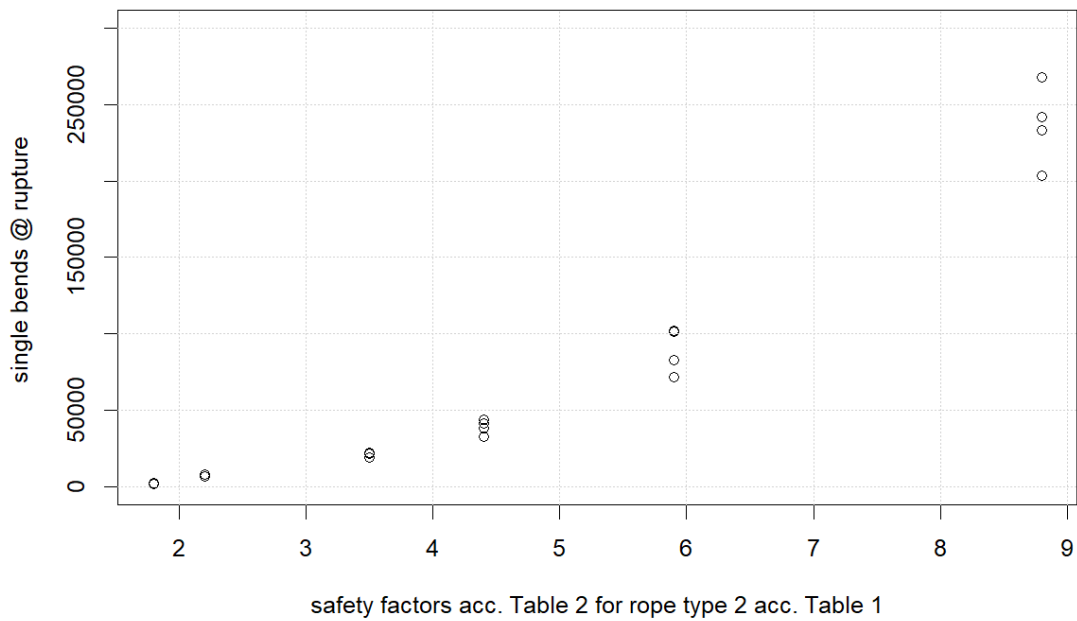


Figure 5: Series 1b, single bends to rupture for rope type 2 at various safety factors

With regard to the variation of the fleet angle, it can be seen that the number of tolerable single bending cycles to rupture decreases with increasing fleet angle (see Figure 6 and Figure 7). This is true for both sheave materials and bending ratios investigated (see Table 2). As expected, it is also clear that N also increases with a larger bending ratio.

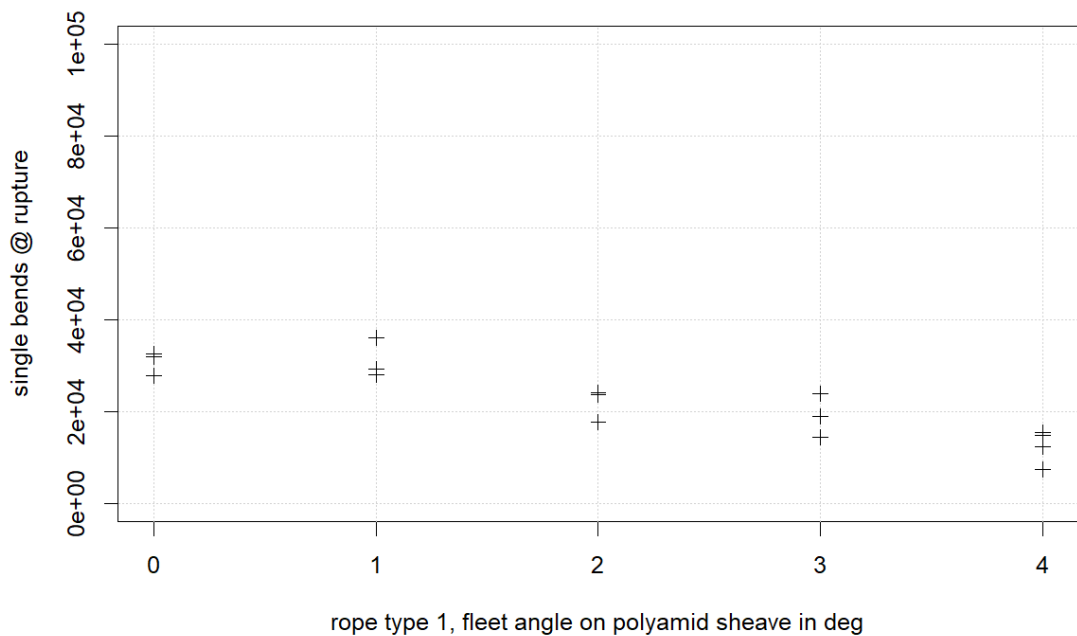


Figure 6: Series 3a, single bends to rupture for rope type 1 at various fleet angles on a polyamide sheave BV = 16.8

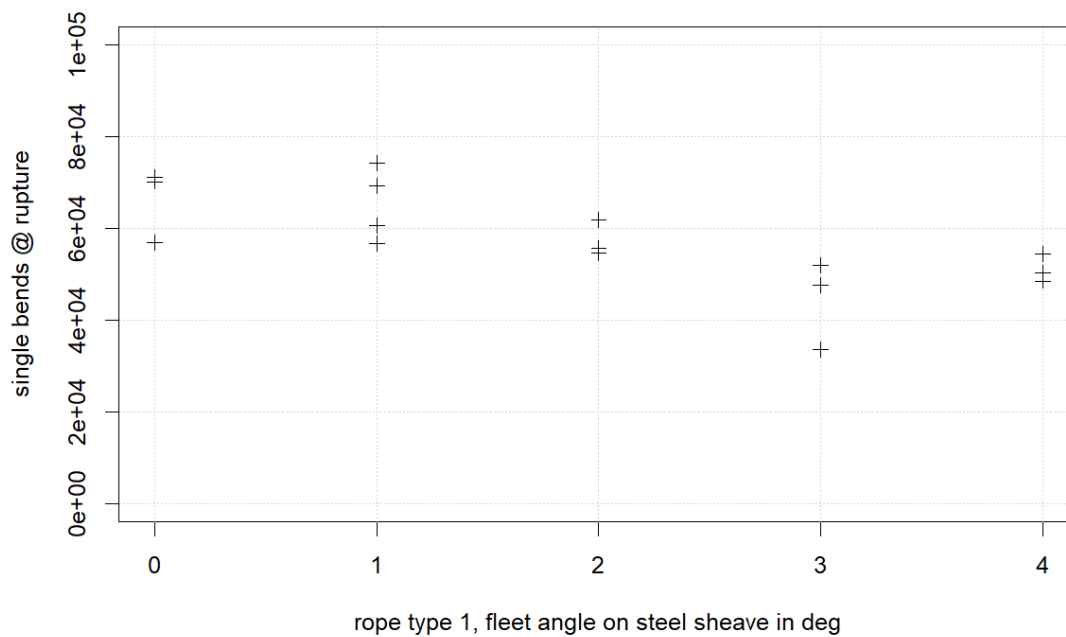


Figure 7: Series 3b single, bends to rupture for rope type I at various fleet angles on a steel sheave BV = 22.5

In various series of measurements in the past it was noticed that polyamide sheaves can tend to show some settling in effects within consecutive CBOS test. In order to give an order of magnitude to this effect, which has not yet been described in the literature, eleven consecutive CBOS tests to failure were carried out on a new polyamide test sheave. It was found that there is a trend. As the number of tests increases, so does the number of single bending cycles that can be endured (see Figure 8). The tests were carried out at a fleet angle of 4°.

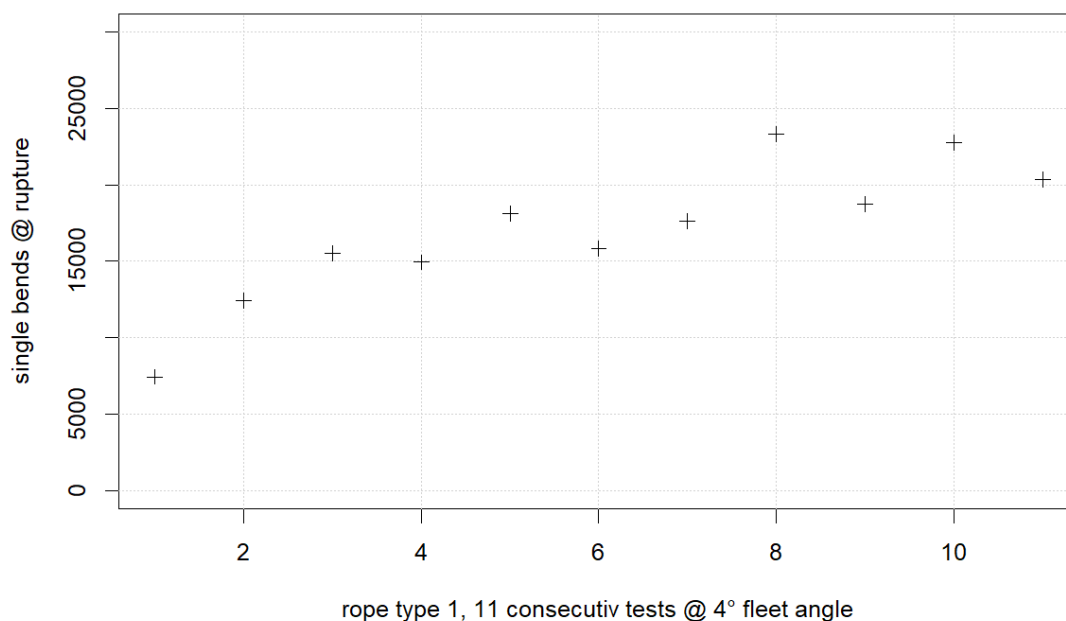


Figure 8: Series 3c, single bends to rupture for rope type I for 11 consecutively carried out CBOS-test on a single polyamide sheave BV = 16.8 at 4° fleet angle

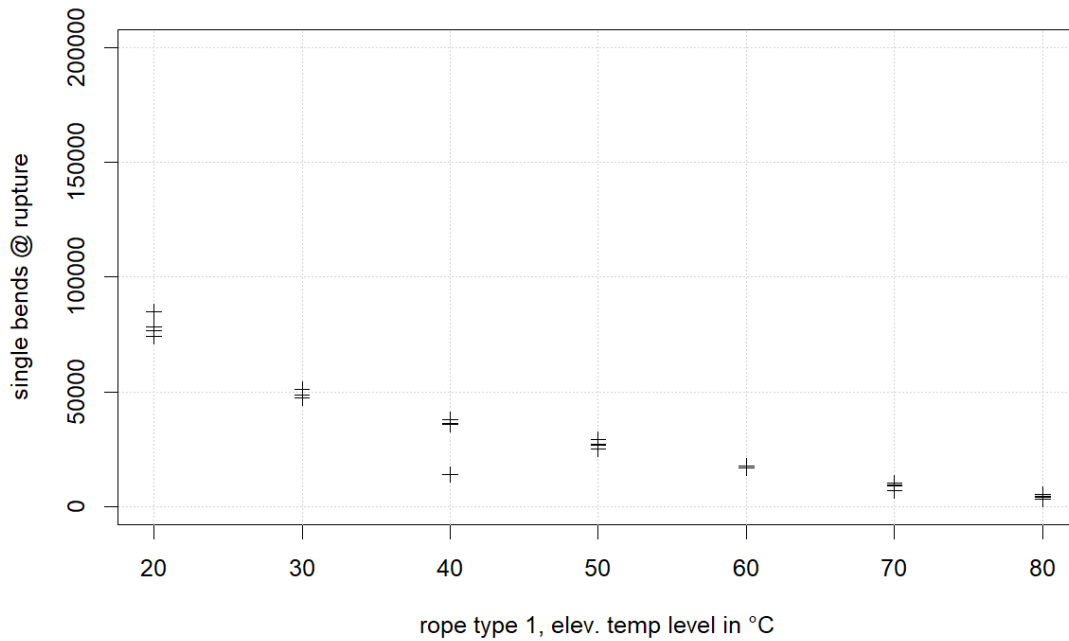


Figure 9: Series 4a, single bends to rupture for rope type 1 at elevated temperatures in the bending zone on a steel sheave

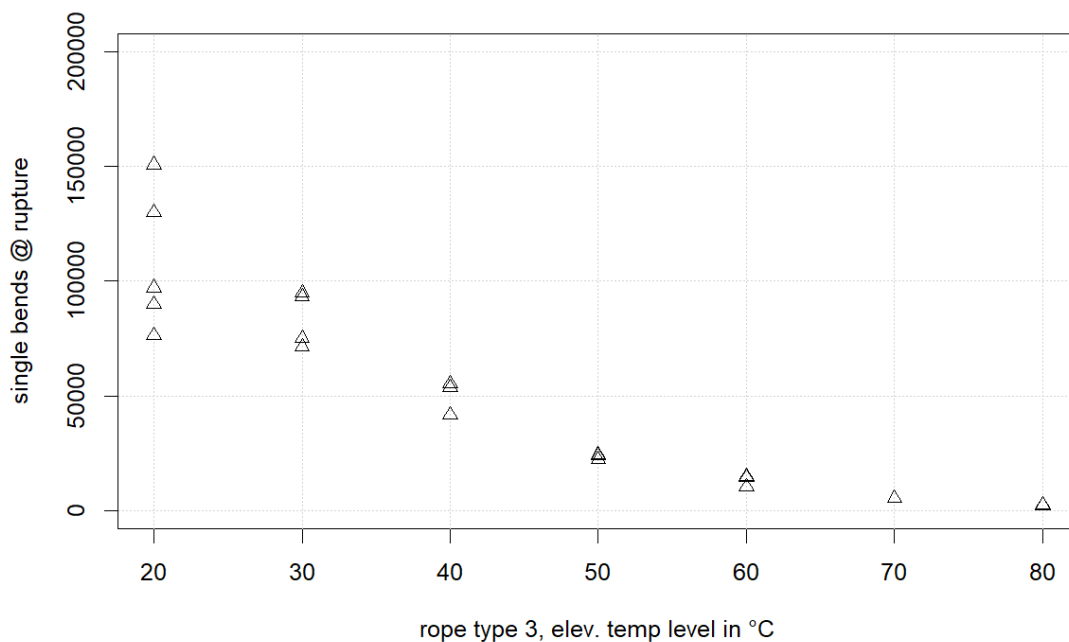


Figure 10: Series 4b, single bends to rupture for rope type 3 at elevated temperatures in the bending zone on a steel sheave

Figure 9 and Figure 10 show the single bending cycles achieved at increased ambient temperature. Here too, the expected trend of decreasing numbers of bending cycles with increasing ambient temperature is confirmed. The factor level 20 °C refers to a test at an uncontrolled ambient temperature. For both rope types, there is a clear decrease in the number of bending cycles until rupture. In both cases, it can be observed that N is close to 0 at high temperatures (a few 100 bends). The safety factors and bending ratios of both test series (for rope types 1 and 3) are almost identical. It can be assumed that N

falls faster with increasing temperature for rope type 3 than for rope type 1. Furthermore, it can be observed that the scatter of the groups is also lower at lower ambient temperatures.

4. Model implementation and discussion

The known service life models for fibre ropes are summarized in [NOV2017]. Because Feyrers service life equation is probably the most commonly used and has only four parameters instead of the seven described by Heinze, it is used for an initial modelling (see Equation 3). The fitting algorithms for non-linear equations itself and the associated difficulties are not dealt with in this paper. However, it should be noted that these methods alone can lead to significant uncertainties when determining the parameter sets (e.g. local optima). In addition, the sensitivities of the various parameters to the smallest changes in the measurement data are sometimes enormous. A statistical comparison of the adjusted parameters between different measurement series is therefore only recommended to a very limited extent. Nevertheless, the fitted parameters in Equation 3 [NOV2017] for the two measurement series are shown in Table 4 for further discussion and also for comparison with values known in the literature. Due to the high similarity of rope types 1 and 2, both measurement series are combined into one for the fitting (see Figure 11).

$$\lg(N) = f(S, D, d) = a_0 + a_1 \cdot \lg\left(\frac{S}{d^2}\right) + a_2 \cdot \lg\left(\frac{D}{d}\right) + a_3 \cdot \lg\left(\frac{S}{d^2}\right) \cdot \lg\left(\frac{D}{d}\right) \quad (3)$$

Table 4: fitted coefficients of Feyrers Formula for Series 1a and b

Coefficients	a0	a1	a2	a3
Series 1a+b	-91.0245	3012.851	36.68033	-968.3989

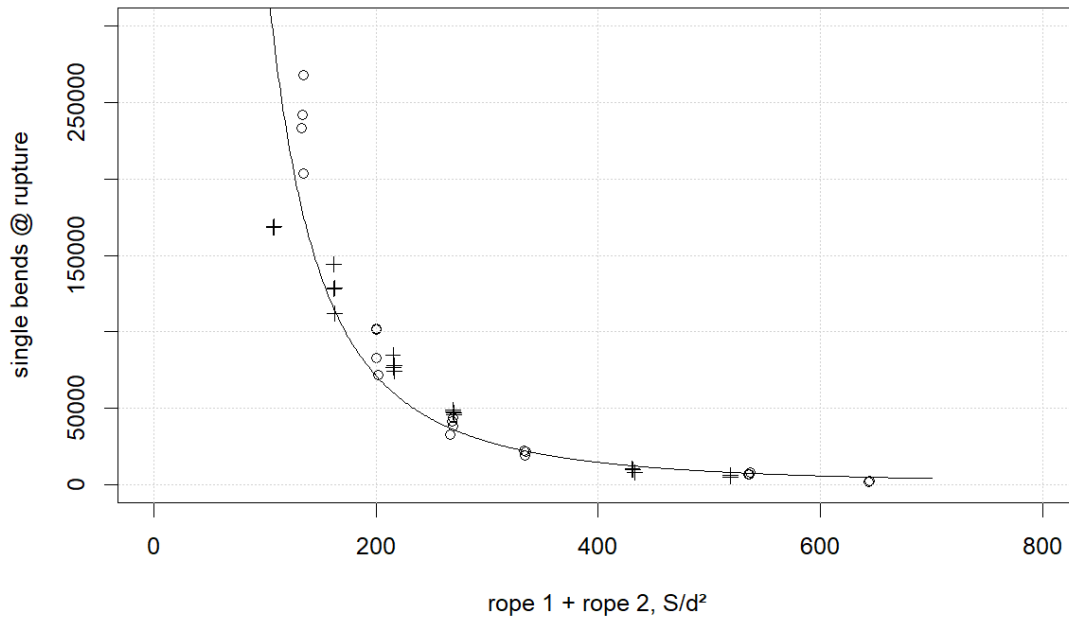


Figure II: Series Ia+b, N over S/d^2 , Feyrers Formula fitted to measured data, linear scaled

For modelling the other factors, only linear models of the form $y(x) = mx + n$ are initially introduced. These models are not necessarily to be regarded as causal / phenomenological models. Rather, they initially only provide an approximation of the recognizable trend behaviour in mathematical form, i.e. they are more quantitative models. Equations 4 to 6 show the respective models of the factors fleet angle, consecutive replications and ambient temperature. The corresponding model parameters are given in Table 5 to Table 7.

$$N(\beta_f) = a_0 + a_1\beta_f; [\beta_f] = \text{deg} \quad (4)$$

Table 5: least squares fitted parameters of model according equation 4

Coefficients	a0	a1
Series 3a (PA-Sheave)	32,839	-4,894
Series 3b (ST-Sheave)	67,405	-5,187

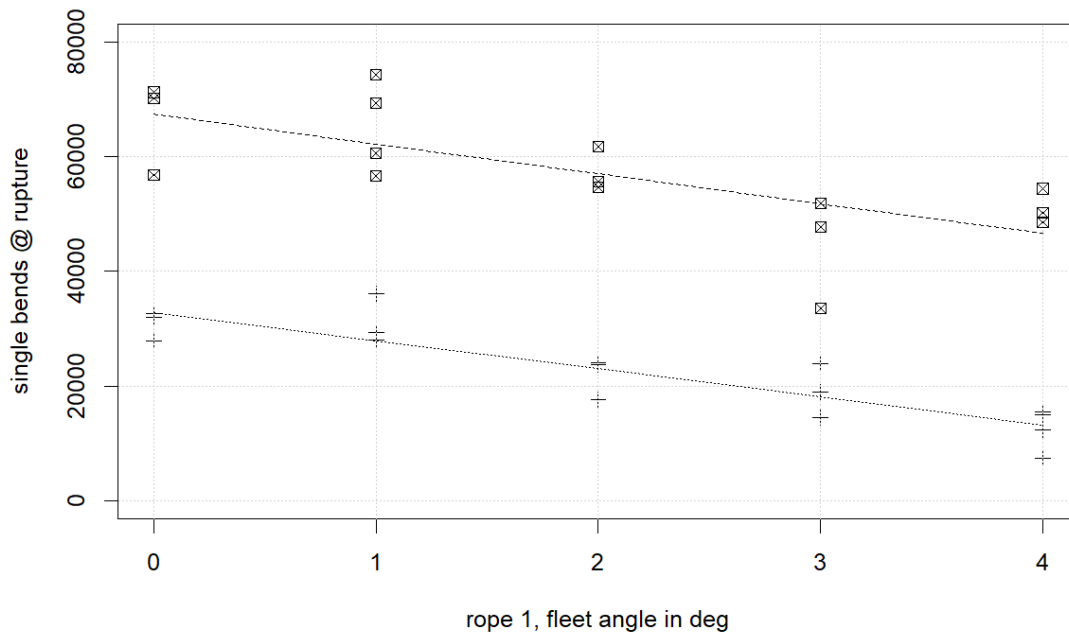


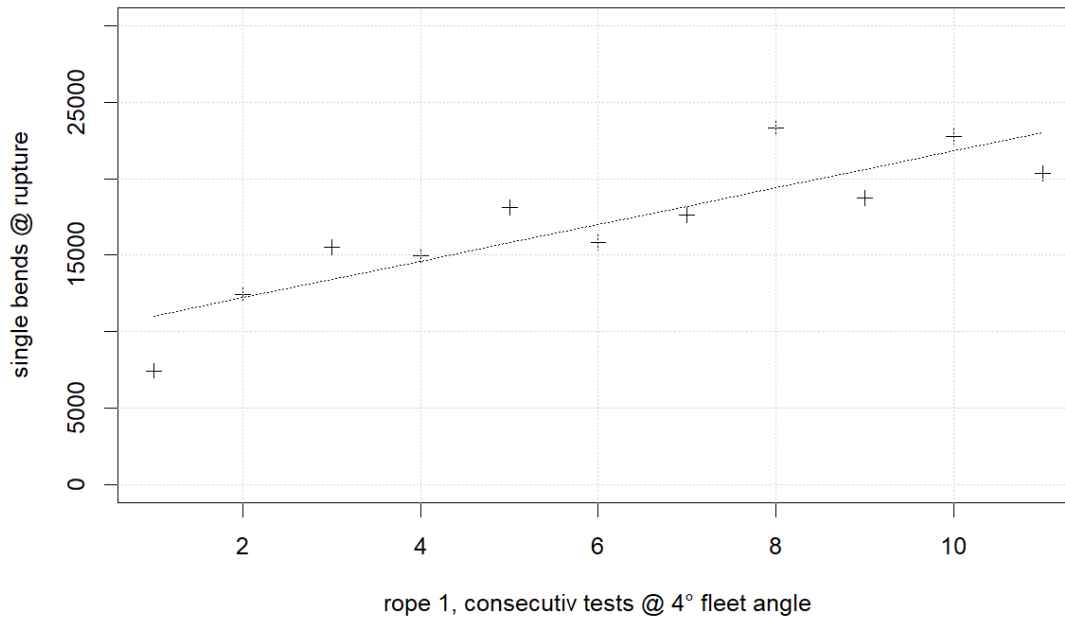
Figure 12: Series 3a and b, linear model for fleet angle

A direct comparison of the measurement series 3a and b for rope type 1 (see **Figure 12**) shows that the rope reacts in the same way to different bending ratios and sheave materials in terms of the reduction in achievable bending cycles due to an increasing fleet angle. For a bending ratio range of 16.8 to 22.5, a reduction in service life of approx. 5,000 single bends per degree of fleet angle can be observed, irrespective of the sheave material. If consecutive tests are carried out, an increase in service life of approx. 1,200 bends per consecutive pass can be seen on polyamide sheaves (see Figure 13).

$$N(Rep) = a_0 + a_1 Rep; [Rep] = 1 \quad (5)$$

Table 6: least squares fitted parameters of model according equation 5

Coefficients	a0	a1
Series 3c (PA-Sheave)	9,826	1,198

**Figure 13:** Series 3c, linear model for consecutive replications (settling in of PA-sheave)

With regard to temperature behaviour, the assessment is less clear (see Figure 15). Both rope types tested, although very similar in design and easily comparable, show differences in their reaction to an increased ambient temperature. The somewhat firmer rope 3 starts at higher values of N at room temperature, but then drops more sharply with increasing temperature than rope 1 (-1,886 bends/10 K). Rope 1, which initially performs somewhat more moderately, starts at only approx. 87,000 bends at room temperature, but then drops more gently to -1,110 bends/10 K. One possible reason for this could be the different coating qualities of the two ropes 1 and 3.

$$N(T) = a_0 + a_1 T; [T] = ^\circ C \quad (6)$$

Table 7: least squares fitted parameters of model according equation 6

Coefficients	a0	a1
Series 4a (rope 1)	86,877	-1,110
Series 4b (rope 3)	136,196	-1,886

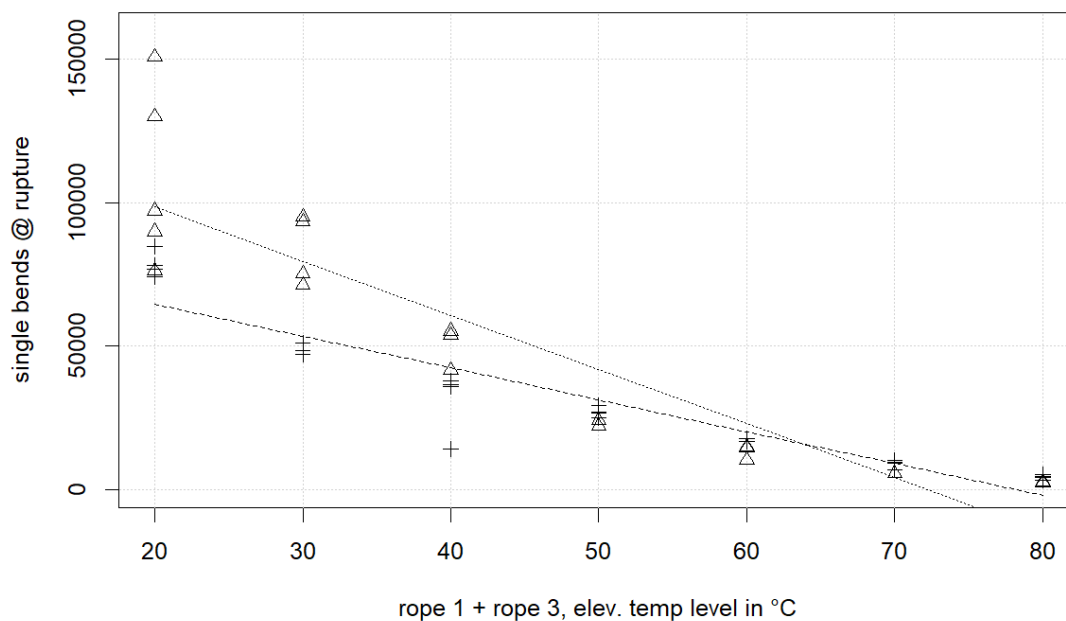


Figure 14: Series 4, linear models for elevated temperature

5. Summary

In summary, the following conclusions can be drawn from the measurements carried out:

- i) All three UHMW-PE ropes tested are comparable, only the coating quality varies. This is particularly important with regard to temperature loads.
- ii) The behaviour of the tested ropes at different safety factors corresponds to the expectation / literature and can be adjusted with different models.
- iii) Polyamide sheaves show no significant influence on the service life in the CBOS test compared to steel sheaves. However, the rope temperature should remain low.
- iv) Braided UHMW-PE ropes react to fleet angles with a reduction in service life and temperature increases in the bending zone.
- v) A settling behaviour can be assumed for PA sheaves. I.e. with increasing service life of the sheaves, ropes run longer on these sheaves.
- vi) With increasing safety factors, the scatter widths within the factor levels increase. I.e. ropes with low loads show a greater fluctuation in their values than ropes with high loads.
- vii) As the ambient temperature decreases, the scatter widths of the groups increase. The behaviour is comparable to point vi). Here, the equivalence of thermal and mechanical stress becomes the focus of safety factors.

6. Acknowledgement

The Authors would like to thank all of the scientific and technical staff at Konecranes and TU Chemnitz who supported the respective test campaign.

References

- [HEI2013] Heinze, T.: „Zug- und biegewechselbeanspruchte Seilgeflechte aus hochfesten Polymerfasern“, Dissertation. Chemnitz 2013
- [MUE2018] Müller, C., Helbig, M., Reimann, N.: „Laufende Faserseile in Anwendungen der Fördertechnik“ – Stand der Forschung, Stuttgarter Seiltage 2018
- [NOV2017] Novak, G.: „Zur Abschätzung der Lebensdauer von laufenden hochmodularen Faserseilen“, Dissertation. Stuttgart 2017
- [ODNI032] M. Meuwissen, R. Bosman, M. Vlasblom, M. Eijssen, S. Leite, S. Bull, O. Haugland, V. Ahjem: “Bending lifetime prediction method for HMPE rope solutions”. Oippec Conference 2024, Bardolino.
- [VOG2004] Vogel, W., Wehking, K.: „Neuartige Maschinenelemente in der Fördertechnik und Logistik: Hochfeste, laufende Faserseile.“ Logistics Journal: nicht-referierte Veröffentlichungen, Vol. 2004.
- [WHR2017] Wehr, M.: „Beitrag zur Untersuchung von hochfesten synthetischen Faserseilen unter hochdynamischer Beanspruchung“, Dissertation. Stuttgart 2017